# Deuterium z-pinch as a powerful source of multi-MeV ions and neutrons for advanced applications

D. Klir, A. V. Shishlov, V. A. Kokshenev, P. Kubes, A. Yu. Labetsky, K. Rezac, R. K. Cherdizov, J. Cikhardt, B. Cikhardtova, G. N. Dudkin, F. I. Fursov, A. A. Garapatsky, B. M. Kovalchuk, J. Krasa, J. Kravarik, N. E. Kurmaev, H. Orcikova, V. N. Padalko, N. A. Ratakhin, O. Sila, K. Turek, V. A. Varlachev, A. Velyhan, and R. Wagner

Citation: Physics of Plasmas **23**, 032702 (2016); doi: 10.1063/1.4942944
View online: http://dx.doi.org/10.1063/1.4942944
View Table of Contents: http://scitation.aip.org/content/aip/journal/pop/23/3?ver=pdfcov
Published by the AIP Publishing



PHYSICS OF PLASMAS 23, 032702 (2016)

# Deuterium z-pinch as a powerful source of multi-MeV ions and neutrons for advanced applications

D. Klir,[1] A. V. Shishlov,[2,3] V. A. Kokshenev,[2] P. Kubes,[1] A. Yu. Labetsky,[2] K. Rezac,[1] R. K. Cherdizov,[2] J. Cikhardt,[1] B. Cikhardtova,[1] G. N. Dudkin,[3] F. I. Fursov,[2] A. A. Garapatsky,[3] B. M. Kovalchuk,[2,3] J. Krasa,[4] J. Kravarik,[1] N. E. Kurmaev,[2] H. Orcikova,[5] V. N. Padalko,[3] N. A. Ratakhin,[2,3] O. Sila,[1] K. Turek,[5] V. A. Varlachev,[3] A. Velyhan,[4] and R. Wagner[5]

[1]*Czech Technical University in Prague, Faculty of Electrical Engineering, Technicka 2, 16627 Prague 6, Czech Republic*
[2]*Institute of High Current Electronics SB RAS, 2/3 Akademichesky Ave., 634055 Tomsk, Russia*
[3]*National Research Tomsk Polytechnic University, 30 Lenina Ave., 634050 Tomsk, Russia*
[4]*Institute of Physics, ASCR, Na Slovance 2, 18221 Prague 8, Czech Republic*
[5]*Nuclear Physics Institute, ASCR, Na Truhlarce 39, 18086 Prague 8, Czech Republic*

(Received 29 September 2015; accepted 16 February 2016; published online 4 March 2016)

A novel configuration of a deuterium z-pinch has been used to generate a nanosecond pulse of fast ions and neutrons. At a 3 MA current, the peak neutron yield of $(3.6 \pm 0.5) \times 10^{12}$ was emitted within 20 ns implying the production rate of $10^{20}$ neutrons/s. High neutron yields resulted from the magnetization of MeV deuterons inside plasmas. Whereas deuterons were trapped in the radial direction, a lot of fast ions escaped the z-pinch along the z-axis. A large number of >25 MeV ions were emitted into a 250 mrad cone. The cut-off energy of broad energy spectra of hydrogen ions approached 40 MeV. The total number of >1 MeV and >25 MeV deuterons were $10^{16}$ and $10^{13}$, respectively. Utilizing these ions offers a real possibility of various applications, including the increase of neutron yields or the production of short-lived isotopes in samples placed in ion paths. On the basis of our experiments with various samples, we concluded that a single shot would have been sufficient to obtain GBq positron activity of $^{13}N$ isotopes via the $^{12}C(d,n)^{13}N$ reaction. Furthermore, the first z-pinch generated neutron radiograph produced by ≈20 ns pulses is presented in this paper. *© 2016 AIP Publishing LLC*. [http://dx.doi.org/10.1063/1.4942944]

## I. INTRODUCTION

At present, z-pinches are known as powerful sources of x-rays.[1] An x-ray power of 200 TW was achieved by an efficient compression and conversion of stored electrical energy into plasmas. A high efficiency of z-pinch generators is not limited to the production of x-rays. Z-pinches and plasma foci are also investigated as portable sources of ions and neutrons for industrial, scientific, and medical applications.[2–7] For most of the contemporary applications, z-pinches cannot be competitors of conventional accelerators such as cyclotrons and RF accelerators. However, there is a niche that z-pinches could occupy and that should be based on a powerful ion pulse of a nanosecond duration. Short, multi-MeV ion pulses can be generated also by ultrashort-pulse laser systems. For instance, laser-driven ions have been used to produce short-lived isotopes[8,9] and neutron beams.[10] In this paper, we therefore aim to demonstrate that z-pinches may eventually be competitive sources of nanosecond ion and neutron pulses.

In the past 10 years, we studied the emission of fusion neutrons in various z-pinch configurations. We researched a deuterated fibre z-pinch,[11] a z-pinch with a neck from microporous deuterated polyethylene,[12] a wire–array z-pinch imploding onto a deuterated fibre,[11] and a deuterium gas-puff z-pinch[13–16] on the S-300 and GIT-12 generators. At the current of 1.5–3 MA, the highest neutron yields on the order of $10^{11}$ were produced in optimized deuterium gas-puff z-pinches.[17] A further increase of neutron yields by one order of magnitude, namely, up to $3.6 \times 10^{12}$, was achieved by a novel configuration of a deuterium gas-puff z-pinch at 3 MA currents.[18,19] On the basis of neutron TOF spectra and other diagnostics, we concluded that the efficient neutron production resulted from the generation of high energy deuterons and probably also from their magnetization inside plasmas.[18] A stack of CR-39 track detectors on the z-pinch axis showed hydrogen ions up to 38 MeV. The observed energies were about five times greater than the maximum deuteron energy observed in previous dense plasma focus and z-pinch experiments.[16,20–23] The energies of hydrogen ions up to 38 MeV were also larger than the applied pinch voltages in the largest pulsed power facilities, and far beyond theoretical predictions and numerical simulations for MA currents.[24] Evidently, the ion acceleration and neutron production in z-pinches are still not well understood (see, e.g., Ref. 25 and references therein). As a result, our recent experiments have been focused on the characterization of ion and neutron emission from the novel configuration of a deuterium gas-puff z-pinch. Whereas the neutron emission was characterized to a large extent in Ref. 19, the basic properties of ion emission are presented in this paper.

In Section II, we describe a novel configuration of a gas-puff z-pinch accelerating a large number of ions to multi-MeV energies. Section III presents the most important parameters of deuterons produced in a deuterium gas-puff, whereas the results obtained with natural hydrogen gas are mentioned in Section IV. The discussion of our experimental results is the subject of Section V. We show that z-pinches exceed many parameters achievable with state-of-the-art laser technology even though they have not been researched to such an extent as laser-based sources. In order to demonstrate the usefulness of z-pinches, Section VI provides two examples of potential applications. The first example is the production of positron-emitting isotopes for nuclear medicine. It seems that the number of fast ions accelerated in a single shot is sufficient for the production of GBq positron activity of $^{13}$N isotopes. The second exemplary application is a neutron radiograph that was obtained with nanosecond pulses generated by our z-pinch. Finally, conclusions are summarized in Section VII.

## II. NOVEL CONFIGURATION OF A DEUTERIUM GAS-PUFF Z-PINCH

Z-pinch experiments with deuterium gas puffs have been carried out on the GIT-12 generator at a 3 MA current and microsecond rise-time.[26] Recently, a novel configuration of a deuterium gas-puff z-pinch has been used to accelerate deuterons and to generate DD fusion neutrons.[18,19] In order to form a homogeneous, uniformly conducting layer at a large initial radius, an inner deuterium gas puff was surrounded by an outer hollow cylindrical plasma shell. The plasma shell consisting of hydrogen and carbon ions was formed at the diameter of 350 mm by 48 plasma guns. A linear mass of the plasma shell was about 5 $\mu$g/cm, whereas a total linear mass of deuterium gas in single or double-shell gas puffs was between 80 and 100 $\mu$g/cm. The implosion lasted ≈700 ns and seemed to be stable up to a 4 mm radius as shown in Fig. 1.

During stagnation, $m=0$ instabilities became more pronounced. When a disruption of necks occurred ($t=0$ ns in Fig. 1, see, e.g., Ref. 25 for more information about disruption), high energy (>2 MeV) bremsstrahlung radiation together with a main neutron pulse was produced. A peak neutron yield reached $(3.6 \pm 0.5) \times 10^{12}$, whereas a dose of >200 keV photons of up to 100 Gy (air kerma) was measured with TLF-700 thermoluminescence dosimeters[27] at 3 cm behind the anode surface. Calculating with a 20 ns duration, we obtain the production rate of $10^{20}$ neutrons/s and $5 \times 10^9$ Gy/s.

In Ref. 18, we demonstrated that high neutron yields resulted from the magnetization of fast deuterons inside plasmas. Whereas deuterons were trapped in the radial direction, a lot of fast ions escaped the z-pinch along the axis. In order to obtain more detailed information about these ions, we have therefore used various diagnostic techniques in our recent experiment. The most important findings are described in Sec. III.

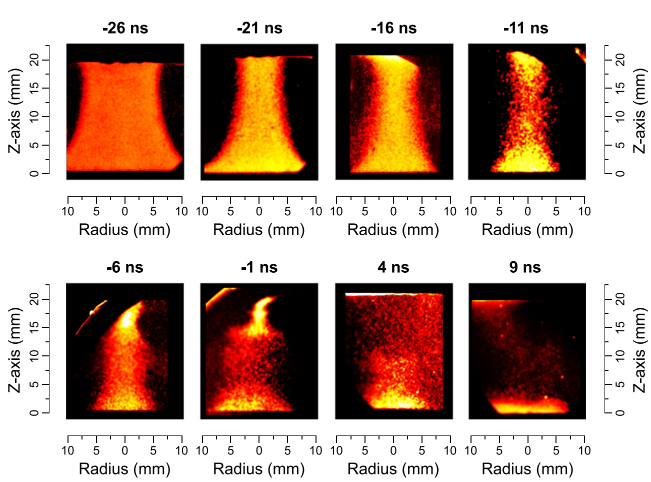


FIG. 1. Gated soft x-ray images of the novel configuration of a deuterium z-pinch. The time $t=0$ corresponds to the disruption accompanied by the sharp onset of >2 MeV bremsstrahlung radiation and the start of main neutron emission. Note: The images were combined from two shots with the implosion time of ≈670 ns.

## III. CHARACTERIZATION OF ON-AXIS IONS

### A. Energies of hydrogen ions

The energies of accelerated ions were measured with the stack of CR-39 solid-state nuclear track detectors. The stack was placed 19 cm below the cathode mesh. Figure 2 shows the scheme of diagnostics and a typical result of deuteron- or proton-induced tracks in the CR-39 detectors.

The analysis of tracks in the shot presented in Fig. 2 showed that all CR-39 layers were saturated by high-energy hydrogen ions. It implied more than $10^{10}$ of >30 MeV hydrogen ions per steradian. An exemplary circular footprint and microphotographs are displayed in Fig. 2(c). On the fifth CR-39 layer, there was no significant difference in the

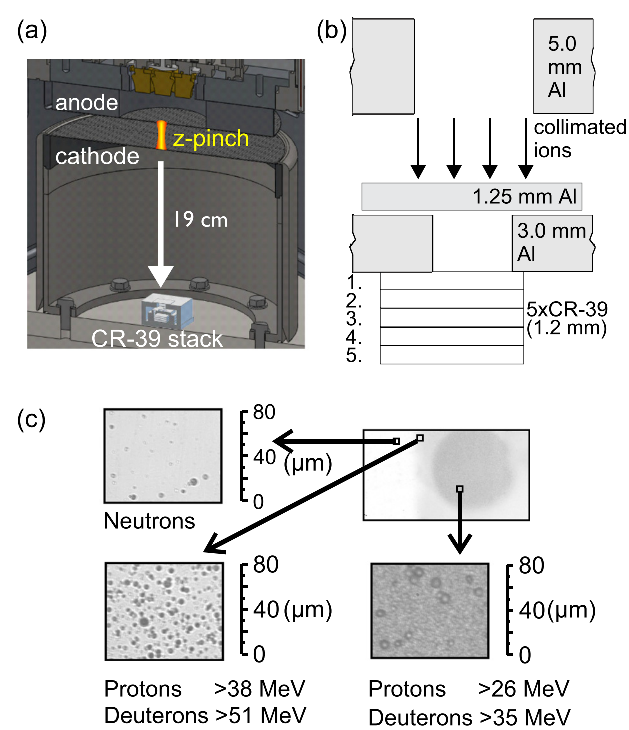


FIG. 2. Measurement of ion energies by the stack of CR-39 track detectors. (a) Scheme of the on-axis diagnostics of ion energies. (b) The stack of CR-39 detectors with aluminum absorbers. (c) Circular footprint on the fourth CR-39 detector with the microphotographs of the proton and/or deuteron-induced tracks etched for 2 h in 30% KOH at 70 °C. Neutron background corresponds to the area of the CR-39 detectors filtered by 9.25 mm of aluminum. Shot No. 1610, $(2.9 \pm 0.3) \times 10^{12}$ neutrons.

number of tracks behind 4.25 mm and 9.25 mm of aluminum. Therefore, these tracks were assigned to neutron-induced recoil protons. As far as the fourth CR-39 detector is concerned, the number of tracks behind 4.25 mm of aluminum was higher than the background created by fast neutrons (see Fig. 2). As a result, these tracks were assigned to fast hydrogen ions and the cut-off energy of broad energy spectra of hydrogen ions was estimated as 40 MeV, i.e., the energy of protons penetrating 4.25 mm of aluminum and 3.6 mm of CR-39 material.

We intended to confirm high-energy deuterons on the axis by another diagnostic technique. For this reason, we placed various samples on the z-pinch axis below the cathode mesh. After a shot, the nuclear activation analysis of these samples was performed with a high-purity Ge detector. In the case of duraluminum and tungsten-copper samples, the $^{27}$Al(d,x)$^{24}$Na and $^{182}$W(d,3n)$^{181}$Re reactions were identified by post-shot gamma-ray spectroscopy indicating an abundance of >15 MeV deuterons on the z-axis (cf. Fig. 3).

The number of ions produced in a single shot was sufficient to activate on-axis samples for several months. Among radionuclides with a half-life of several months, we observed isotopes of cobalt and magnesium which were produced by reactions of fast deuterons with the cathode mesh, namely, by $^{56}$Fe(d,n)$^{57}$Co, $^{56}$Fe(d,2n)$^{56}$Co, $^{56}$Fe(d,$\alpha$)$^{54}$Mn reactions. The isotopes of $^{57}$Co, $^{56}$Co, and $^{54}$Mn have the half-lives of 272 days, 77 days, and 312 days, respectively.

The abundance of multi-MeV ions caused that the experimental chamber was activated after each shot. Therefore, we let the experimental chamber cool down, and we opened it the following day. It prevented us from characterizing the ion flux by the detection of short-lived radioisotopes with a low-energy threshold and with a half-life in minutes.[30] In order to estimate the total number of fast deuterons, we used therefore the procedure that is described in Subsection III B.

### B. Total number of multi-MeV deuterons

Our previous z-pinch experiments with deuterium gas-puffs were focused on neutron production (see, e.g., Ref. 18). Therefore, to obtain the information about deuterons, we took advantage of our comprehensive neutron diagnostics[19] and we characterized the escaping ions via neutron-producing reactions.

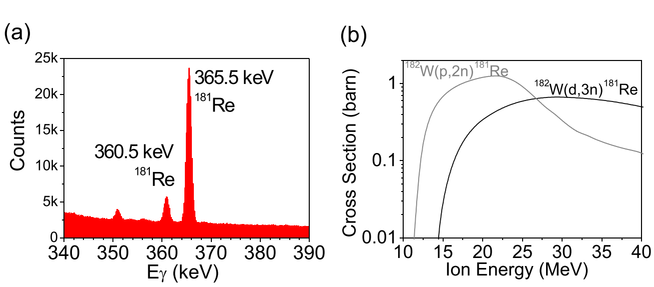


FIG. 3. (a) Gamma-ray spectrum of a copper-tungsten sample placed 10 cm below the cathode mesh and activated by fast deuterons in shot No. 1691, $(2.1 \pm 0.3) \times 10^{12}$ neutrons. (b) Energy dependence of the $^{182}$W(d,3n)$^{181}$Re reaction cross-section.[28] The half-live of $^{181}$Re isotopes is 19 h. Note: $^{181}$Re isotopes can be produced also by the $^{182}$W(p,2n) reaction with a somewhat lower threshold.

In order to distinguish primary DD neutrons from secondary neutrons produced in a sample, we decided to use lithium fluoride. We placed a $3 \times 3\,\text{cm}^2$ square sample onto the axis 3 mm below the cathode mesh. As shown in Fig. 4, the catcher with a natural abundance of $^7$Li isotopes significantly increased a total neutron yield (up to $6 \times 10^{12}$) and changed a neutron spectrum. According to a BDS-10000 super-heated fluid detector,[29] the number of neutrons between 10 and 20 MeV was increased by one order of magnitude up to $(5 \pm 1) \times 10^{11}$. Most of these neutrons originated from the $^7$Li(d,n) reaction with the $Q$-value of 15.03 MeV. However, the residual nuclei of this reaction often remain in excited states and three-body processes, e.g., $^7$Li(d,n + $\alpha$)$^4$He, contribute to neutron production. Consequently, >10 MeV neutrons formed approximately a quarter of the neutron yield produced by the LiF catcher (see, e.g., Fig. 4(b) or Ref. 31). Calculating with $5 \times 10^{11}$ of >10 MeV neutrons, the LiF catcher produced approximately $(2.0 \pm 0.5) \times 10^{12}$ neutrons. When the number of neutrons from the LiF catcher is known, it is possible to better characterize the ion flux. The total number of deuterons

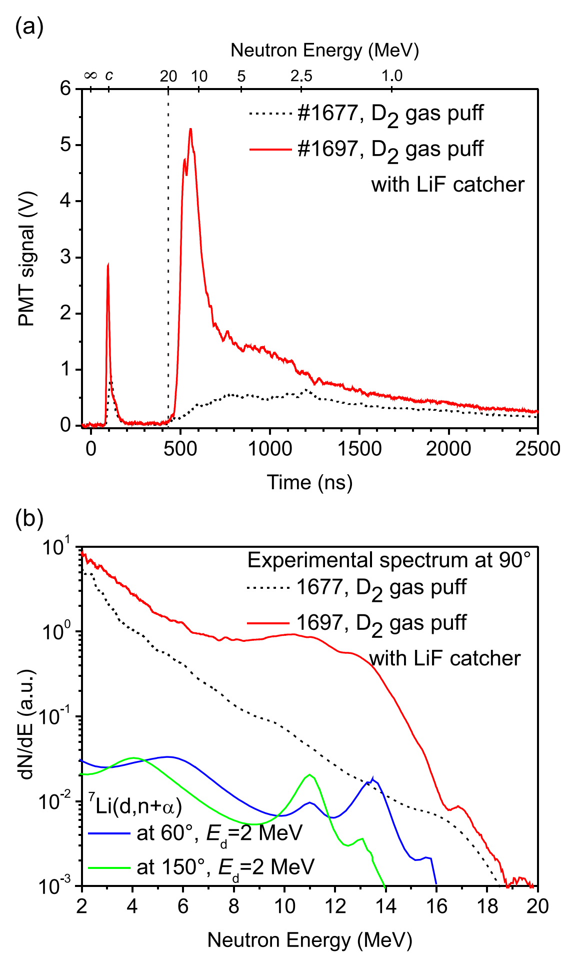


FIG. 4. (a) Radial neutron time-of-flight signal at 25.7 m in the shots without a catcher (dotted black line, shot No. 1677, $3.2 \times 10^{12}$ neutrons) and with a LiF catcher (solid red line, shot No. 1697, $6 \times 10^{12}$ neutrons). The relative scale of the y-axis is the same for both waveforms. When interpreting the ToF signals, the sensitivity of the ToF detector to neutrons with different energies had to be taken into consideration. (b) Experimental radial neutron energy spectra in the shots with and without a LiF catcher; theoretical neutron spectra of the $^7$Li(d,n + $\alpha$)$^4$He reaction for 2 MeV deuterons and two observation angles of 60° or 150° with respect to incident deuterons.[28]

interacting with the LiF catcher $N_d$ can be estimated from the number of neutrons $N_{LiF}$, thick-target yield $Y_{LiF}(E_d)$, and deuteron energy spectra $f(E_d)$ as

$$N_d = \frac{N_{LiF} \int f(E_d) dE_d}{\int f(E_d) Y_{LiF}(E_d) dE_d}. \quad (1)$$

If we use the LiF thick-target yield from Fig. 5 and the approximate distribution of deuteron kinetic energy deduced from DD neutron spectra $f(E_d) = dN_d/dE_d \propto E_d^{-2}$ (cf. Ref. 19), we find out that $10^{16}$ deuterons above 1 MeV collided with the LiF catcher and that the total energy carried by >1 MeV deuterons approached 5 kJ. There is some uncertainty since the spectrum of deuterons interacting with the catcher was not measured directly and since the thick-target yield could be influenced by different stopping power in target-ablation plasmas.[32] It is also necessary to take into account that our z-pinch was optimized with respect to high neutron yields from deuterium plasmas and that the number of shots with a LiF catcher was quite low. Therefore, it is possible that the number and/or energies of deuterons interacting with a catcher can be increased in future experiments.

### C. Duration of ion pulses

The LiF catcher was used not only to estimate the total number of on-axis ions but also to measure the duration of an ion pulse. It was difficult to measure the ion pulse duration by standard methods (e.g., with (p,$\gamma$) reactions, Faraday cups, Rogowski coils, and *dB*/*dt* loops) because of strong >2 MeV bremsstrahlung background, ion beam neutralization in deuterium gas, and harsh electromagnetic environment inside the experimental chamber. Therefore, we tried to convert deuterons to neutrons by a catcher and to measure pulse durations by our neutron time-of-flight detectors. To measure the time of neutron production, it was necessary to place one time-of-flight detector as close to the neutron source as possible. However, even at 2 m, the time-of-flight signal is strongly dispersed due to a very wide neutron energy spectra from our deuterium gas-puff (cf. shot No. 1677 in Fig. 4). Fortunately, the nuclear reactions of deuterons with $^7$Li isotopes produced the radial neutron peak between 10 and 14 MeV as shown in Fig. 4. At a 2 m distance, the dispersion of this neutron peak of about 7 ns was on the order of temporal resolution of our detectors.[33] Fig. 6 shows the exemplary result from two shots with the shortest and the longest ion emission. When the dispersion of the main neutron peak and the tail formed by <10 MeV neutrons are taken into account, we obtain the FWHM of ion pulses between 10 and 30 ns. Calculating with the average value of 20 ns and with $10^{16}$ fast deuterons, we find out that the current of >1 MeV deuterons was on the order of 100 kA. Fig. 6 indicates that there was some correlation between neutron emission and bremsstrahlung radiation. This indication was supported by the measurements of neutron yields and doses of bremsstrahlung radiation. A nice correlation between the number of neutrons and the number of >200 keV photons is shown in Fig. 7. This is an important result since the correlations imply that acceleration of electrons was closely connected with ion acceleration mechanism which is still a source of debate.

### D. Ion emission anisotropy

In the preceding paragraphs, we presented the energy and number of deuterons escaping the z-pinch along the axis. To characterize further the escaping deuterons, it was desirable to measure the angular distribution of ion emission. For this purpose, we placed large samples of CR-39 detectors and HD-V2 GafChromic films at 19 cm below the cathode

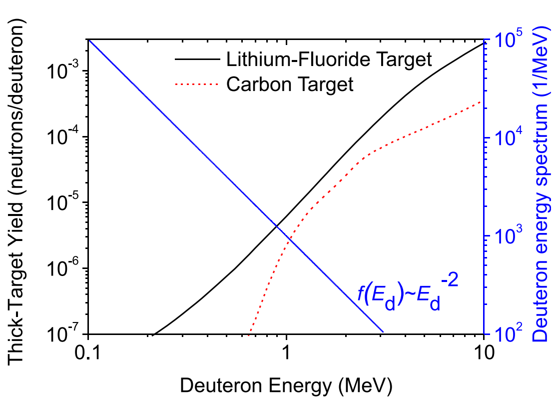


FIG. 5. Thick-target neutron yields from LiF (solid black line) and graphite (dashed red line), the distribution of deuteron kinetic energy (solid blue line). Thick-target yields were calculated from ENDF and SRIM databases[28,34] using the procedure described in Ref. 30.

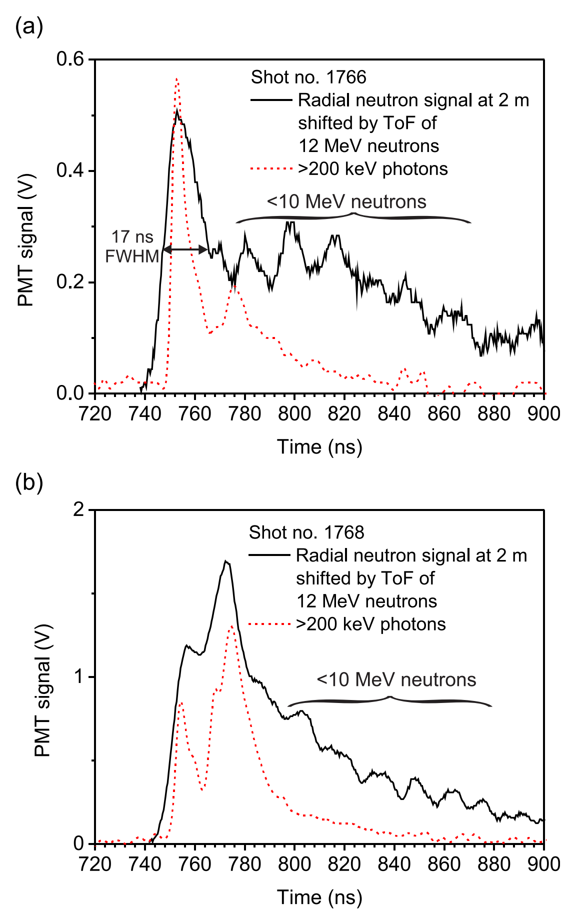


FIG. 6. Neutron ToF signal at 2 m (solid black line) and bremsstrahlung radiation measured by a hard x-ray diode in the radial direction (dashed red line). A $1.4 \times 1.4$ cm$^2$ LiF sample was placed 3 mm below the cathode mesh. (a) Shot No. 1766. (b) Shot No. 1768.

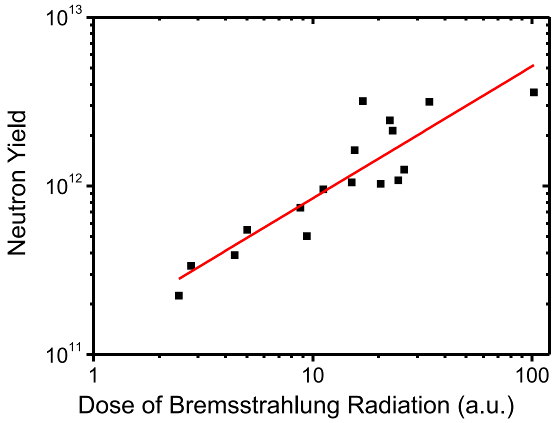


FIG. 7. The correlation of neutron yields with the dose of >200 keV photons measured by a hard x-ray diode in the radial direction. Shots with deuterium gas-puffs without any catcher.

mesh. In Fig. 8, you can see an exemplary result of deuteron- and proton-induced signals at the detectors. If we assume that the radiation dose at the calibrated HD-V2 films was given by deuterons and that the average energy deposited by one deuteron in an active layer was 0.1 MeV (cf. Fig. 8(b)), we will find out that the total number of >25 MeV deuterons was about $10^{13}$. A similar estimate was made by the analysis of the CR-39 detectors. Nevertheless, $10^{13}$ is only a rough estimate of the number of >25 MeV deuterons. Firstly, the number of the fastest deuterons varied strongly from shot to shot. Secondly, our detectors gave the information about a solid angle of 0.8 sr only. Thirdly, the average energy deposited by one deuteron depends on the energy spectrum. Finally, a linear energy transfer (LET) effect has to be taken into account.[35]

As shown in Fig. 8, the emission of 25 MeV deuterons (or 20 MeV protons) was quite collimated since a large number of ions were emitted into a cone with an opening angle of $2\theta = 250$ mrad (assuming a localized ion source and neglecting any focusing effect on emitted ions). On the basis of the measurement in several shots, it was evident that the ion emission was azimuthally asymmetric. Usually, the ion beam divergence was higher in one direction. Another interesting feature was the detection of relatively long (up to 10 cm) and very thin (sub-millimeter) lines. It does not seem probable that such thin lines could be produced by radial electric fields. A more realistic hypothesis is that ions from a point source were dispersed by magnetic fields in the z-pinch. In this respect, it was highly desirable to know if the source of 25 MeV deuterons was so localized. For this reason, we measured the spatial distribution of ion source as described in the following paragraphs.

### E. Spatial distribution of multi-MeV ion source

In order to obtain information about the spatial distribution of an ion source, we placed an ion pinhole camera on the z-pinch axis below the cathode mesh. The scheme of the experimental set-up and exemplary results are shown in Fig. 9.

In the case of the deuteron energy above 17 MeV, the axial ion pinhole camera detected several localized spots as was expected from the measurement of ion emission anisotropy. The spot diameter of about 1.3 mm was at the resolution limit of the ion pinhole camera.

The ion pinhole camera also recorded images of ions with energies below 15 MeV. At these energies, the influence of magnetic fields on ion trajectories is even more important and should be taken into account. Therefore, the interpretation of ion pinhole images below 15 MeV requires an in-depth analysis. This will be the subject of our future work.

## IV. OPTIMIZATION OF HYDROGEN GAS PUFF

The above-mentioned results indicate that megaampere gas-puff z-pinches are able to accelerate deuterons to multi-MeV energies. Naturally, it could be asked if it is also

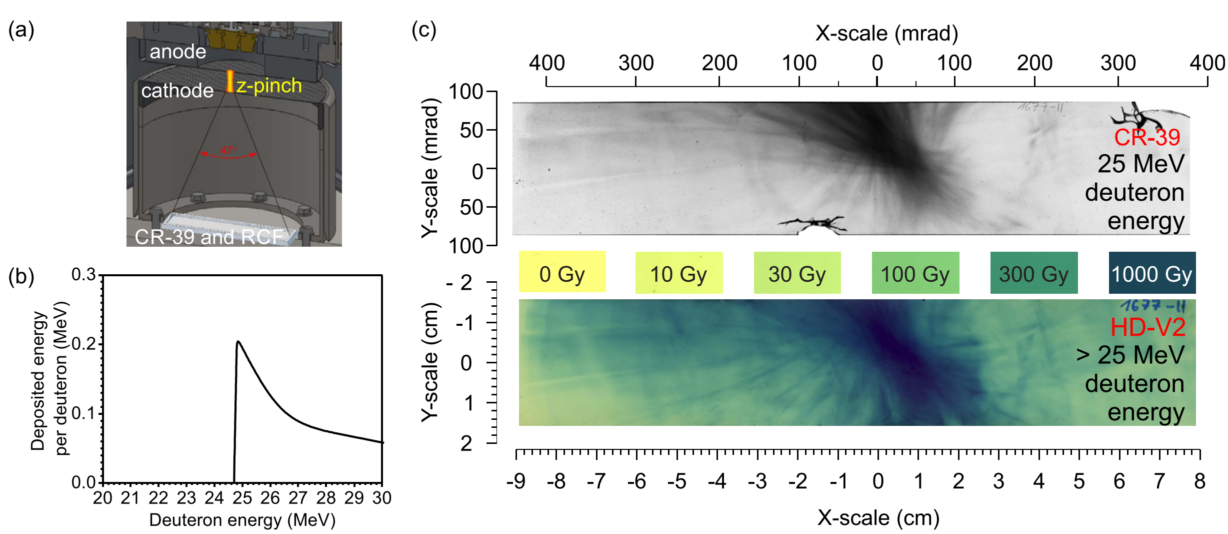


FIG. 8. Measurement of ion emission anisotropy. (a) Scheme of the on-axis diagnostics of anisotropy measurement. The stack consists of a duralumin absorber (1.1 mm), the first CR-39 layer (1.1 mm), a HD-V2 gafchromic film (0.1 mm), and the second CR-39 layer (1.1 mm). (b) The energy deposited by one deuteron in the active layer of the HD-V2 film calculated with the TRIM code.[34] (c) The images detected by the HD-V2 film and the second CR-39 detectors in shot No. 1677, $(3.2 \pm 0.5) \times 10^{12}$ neutrons. In this particular shot, 33 MeV neutrons were measured by an axial neutron ToF detector and many $^{24}$Na isotopes from the $^{27}$Al(d,x)$^{24}$Na reaction were identified by post-shot gamma-ray spectroscopy. Therefore, it is possible that a large number of ≈30 MeV deuterons were produced and that the pattern in the images was created by fast deuterons.

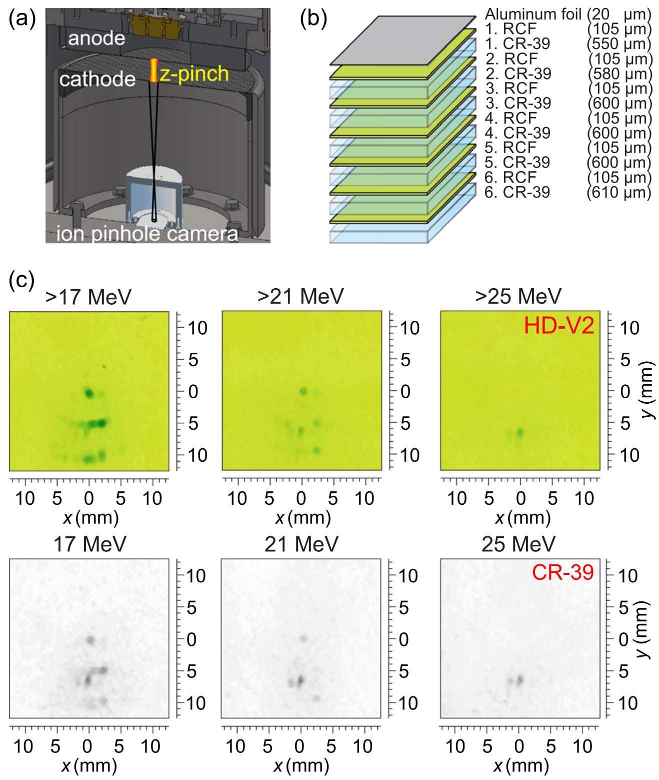


FIG. 9. Measurement of the spatial distribution of the ion source. (a) Scheme of the axial ion pinhole camera with the magnification of 0.6 and the pinhole diameter of 0.5 mm. (b) The stack of 6 pairs of RCF and CR-39 detectors in shot No. 1770. (c) The ion pinhole images detected by the third, fourth, and fifth pair of RCF and CR-39 detectors in shot No. 1770, $(1.7 \pm 0.4) \times 10^{12}$ neutrons. Spatial scales correspond to the plane of the cathode mesh.

possible to accelerate ions by a z-pinch operating with a different gas? If so, then the following question is what the optimal conditions are? In order to answer these questions, we replaced deuterium by natural hydrogen gas. On the basis of our previous research, we expected that gas-injection time played an important role because the spread of gas at large distances made the current concentration onto the axis more difficult.[16,18] Therefore, we carried out several shots with various gas-injection times, whereas the parameters of the GIT-12 generator and the plasma guns remained the same as in the shots with deuterium gas puffs. The expansion of hydrogen gas is faster than deuterium gas by a factor of $v_{H_2}/v_{D_2} \propto \sqrt{m_{D_2}/m_{H_2}} \doteq \sqrt{2} \doteq 1.4$. Indeed, the highest neutron yield with hydrogen gas was observed in the shot when the injection time optimal for deuterium was reduced 1.4-times, i.e., from 300 $\mu$s to 220 $\mu$s. At the 220 $\mu$s injection time, the total linear mass of hydrogen gas was only $\approx$30 $\mu$g/cm, and the stagnation occurred 100 ns earlier at a lower current of about 2.3 MA. It should be mentioned that the number of natural hydrogen molecules for $\hat{m}_{H_2} \approx 30$ $\mu$g/cm is the same as the number of deuterium molecules for $\hat{m}_{D_2} \approx 60$ $\mu$g/cm. Therefore, taking the current $I$ and the atomic number $A$ into account, the electron drift velocity at stagnation $u_e \propto A I_{stag}/\hat{m}$ could be similar in both cases, i.e., with deuterium as well as with natural hydrogen gas puff.

When the hydrogen gas-puff z-pinch was optimized, we observed analogical results to deuterium gas. The implosion seemed to be stable up to a 4 mm radius. During stagnation, $m = 0$ instabilities developed and, when a disruption of necks occurred, the plasma impedance exceeded 0.35 Ω. The high energy (>2 MeV) bremsstrahlung radiation was generated together with high-energy protons. Maximum proton energies of 20 MeV were observed by the stack of RCF and CR-39 detectors (cf. scheme in Fig. 2). Fig. 10 shows a radial neutron spectrum and a CR-39 detector with etched tracks induced by fast protons. Interestingly, the hydrogen gas-puff z-pinch produced a relatively high yield of $10^{11}$ neutrons per shot. In the case of natural hydrogen gas, most of the neutrons were generated by the interaction of fast protons with the cathode mesh or with the experimental chamber. Therefore, neutron yields as well as the radioactivity of the experimental chamber after a shot were good indicators of great numbers and high energies of accelerated protons.

## V. OTHER POWERFUL SOURCES OF MULTI-MEV IONS

In Sections III and IV, we have presented several important parameters of ion pulses generated by the novel configuration of the gas-puff z-pinch. We showed that the deuterium gas-puff z-pinch at the 3 MA current is able to accelerate hydrogen ions up to 38 MeV energies. This is an unprecedented energy which is several times greater than the maximum energies observed in previous z-pinch and plasma focus experiments (cf. Refs. 20 and 37). The total number of >1 MeV and >25 MeV deuterons were $10^{16}$ and $10^{13}$, respectively. High-energy ions were quite collimated since a large number of >25 MeV deuterons were emitted into a 250 mrad cone. The ion pulse seemed to be closely correlated with >200 keV bremsstrahlung radiation and lasted for about 20 ns. The total current of >1 MeV deuterons approached 100 kA.

At this point, it might be interesting to mention other powerful sources of multi-MeV ions. In the past 15 years,

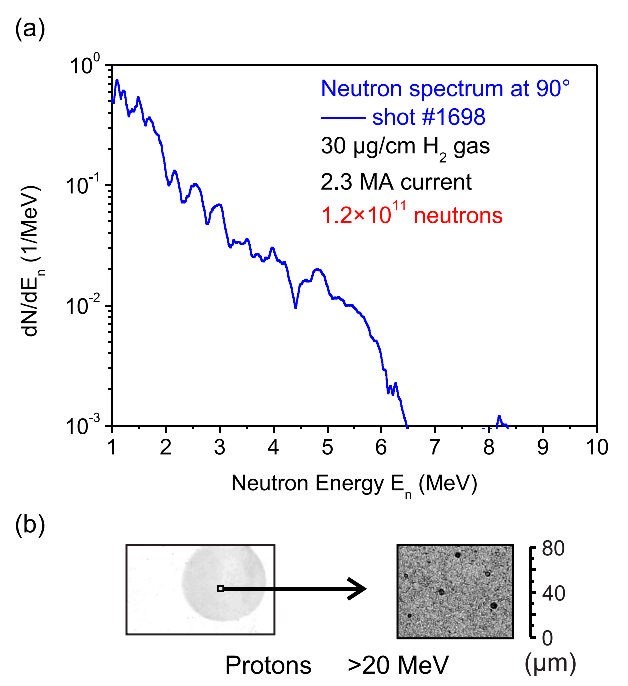


FIG. 10. Experimental results with the hydrogen gas-puff z-pinch in shot No. 1698, $(1.2 \pm 0.2) \times 10^{11}$ neutrons. (a) Radial neutron energy spectrum. (b) Circular footprint on the second CR-39 detector with the microphotograph of the proton-induced tracks etched for 2 h in 30% KOH at 70 °C.

ion acceleration was extensively researched on intense ultrashort-pulse laser systems (see, e.g., Refs. 38–40 and references therein). Recently, successful acceleration of deuterons has been achieved on the VULCAN[41,43] and Trident[10,44] lasers. On the Trident laser, very efficient BOA (break out afterburner) mechanism accelerated $5 \times 10^{11}$ deuterons with a >15 MeV energy into a 250 mrad cone.[10] The comparison of these ultrashort-pulse lasers with our z-pinch-based source could be somewhat misleading since the parameters of the generators as well as the properties of ion emission differ significantly. Nevertheless, when looking on ion numbers and energies only, our results clearly demonstrate how attractive a z-pinch as an ion source could be. In addition to that, ion acceleration in gas-puff z-pinches has not been studied to such an extent as in laser-target interaction. Therefore, there is a chance that z-pinch experiments can be optimized and above-mentioned results can be exceeded in the near future.

For completeness, mention should be made of pinched-beam ion diodes. In the 1980 s, intense pulsed ion beams were researched as inertial-confinement-fusion drivers (see, e.g., Refs. 45 and 46 for more details). Published data about deuteron beams are rather scarce, but there is some information about experiments focused on proton acceleration. One of the most successful experiments was carried out on the Aurora pulsed-power generator which was able to accelerate $5 \times 10^{16}$ protons up to 5 MeV energies.[47] A 160 ns FWHM pulse implied an ion current of about 50 kA. The ions appeared to originate primarily from a small area (2–4 cm$^2$) at an anode. More recently, a pinched-beam ion diode has been fielded on the Mercury pulsed-power machine with a shorter (50 ns) pulse duration at 3.5 MV.[48] Even higher voltage of 6 MV was applied in experiments with Hermes III.[49] Evidently, the 38 MeV peak energy of hydrogen ions in our experiment was significantly higher than the energy achieved with high-voltage ion diodes even though the initial voltage applied on the GIT-12 was lower by one order of magnitude than on the Mercury or Hermes III generators.

A meaningful comparison of various ion sources would require a detailed discussion of many physical and technical parameters. Since the above-mentioned ion sources and experiments differ substantially from each other, it is not easy to find common quantities in literature. Nevertheless, we attempted to find some common quantities and we list the most important ones in Table I. As shown in Table I, each of these powerful ion sources has unique properties with respect to parameters of ion emission. In a simplified way, we can say, that the basic parameters of our gas-puff z-pinch lie somewhere between values achieved with state-of-the-art lasers and powerful pinched-beam ion diodes.

The unique parameters of a z-pinch-based ion source imply a possibility of traditional as well as innovative applications. Two exemplary applications are described in Sec. VI.

## VI. APPLICATIONS OF DEUTERIUM GAS-PUFF Z-PINCHES

### A. Production of positron-emitting radioisotopes

One of the traditional applications of multi-MeV ion sources is the production of positron-emitting radioisotopes

TABLE I. Basic parameters of different powerful sources of multi-MeV protons or deuterons. Some values were estimated or calculated on the basis of data presented in references.

| Driver | Z-pinch | Laser | Laser | Ion diode | Ion diode | Ion diode |
|---|---|---|---|---|---|---|
| Facility name | GIT-12 | Trident | Vulcan | Aurora | Mercury | Hermes-III |
| Reference | This work | 10 and 44 | 41 | 47 | 48 | 49 |
| Ion species | Deuterons | Deuterons | Deuterons | Protons | Protons | Protons |
| Ion spectrum | Broad | Broad | Broad | Quasi-monoenergetic | Quasi-monoenergetic | Quasi-monoenergetic |
| Cut-off energy (MeV) | 38 | 100 | 15 | 5 | 4 | 6 |
| Number of >25 MeV ions in cone with $2\theta = 250$ mrad | $3 \times 10^{12}$ | $10^{11}$ | | | | |
| Number of >1 MeV ions | $10^{16}$ | | $10^{13}$ | $5 \times 10^{16}$ | $2 \times 10^{16}$ | $(1-2) \times 10^{16}$ |
| Total energy of >1 MeV ions (kJ) | 5 | | 0.01 | 40 | 10 | 10 |
| Tunability of ion energies | Difficult | Difficult | Difficult | Possible | Possible | Possible |
| Duration of ion pulse (ns) | 10–30 | 0.001 | 0.001 | 160 | 50 | 40 |
| Tunability of pulse duration | Difficult | Difficult | Difficult | Possible | Possible | Possible |
| Ion current (kA) | 100 | | 1000 | 50 | 60 | 60 |
| Spatial distribution of ion source | Many spots inside 2 cm diameter | 50 $\mu$m diameter | 100 $\mu$m diameter | 2 cm diameter | Many spots inside 5 cm diameter | Many spots |

used in nuclear medicine. In the past 15 years, several laser and plasma focus experiments were carried out to obtain high activity of $\beta+$ emitting nuclei after the bombardment of different materials with fast ions (e.g., Refs. 3, 8, 9, 42, and 50–52). The peak activities of the order of 100 kBq were 4 orders of magnitude lower than the value needed for a clinical positron emission tomography (PET) scan. Therefore, it would be interesting to know the activity that can be reached by ions accelerated in the deuterium gas-puff z-pinch.

The parameters of the deuteron pulse on the GIT-12 generator seem to be convenient for the production of $^{13}$N isotopes via the $^{12}$C(d,n)$^{13}$N reactions. $^{13}$N isotopes with a 10 min half-life are often used for PET myocardial perfusion imaging.[53] As was mentioned at the end of Section III A, the radioactivity inside the experimental chamber did not allow us to analyze short-lived isotopes with a half-life in minutes. Nevertheless, we are able to make reasonable quantitative predictions for deuteron bombardment of graphite on the basis of our experiment with the lithium-fluoride catcher (see Section III B).

The thick-target neutron yields for lithium fluoride and for graphite are displayed in Fig. 5. The convolution of our high-energy tail $f(E_{\rm d}) = dN/dE_{\rm d} \propto E_{\rm d}^{-2}$ with the thick-target yield $Y(E_{\rm d})$ is 4.5-times smaller for graphite than for lithium fluoride. This ratio is not highly sensitive to the power law index $k$ in the high-energy tail dependence $f(E_{\rm d}) = E_{\rm d}^{-k}$. On the basis of the 4.5($\pm$0.5) ratio and $(2.0 \pm 0.5) \times 10^{12}$ neutrons from the LiF sample, we may conclude that our deuteron pulse would produce $(4.5 \pm 1.5) \times 10^{11}$ radioactive nitrogen isotopes. Calculating with the half-life of 598 s, we obtain $(0.8 \pm 0.3)$ GBq activity shortly after the deuteron bombardment. Such activity is supposed to be sufficient for a clinical PET scan.[54] Even though it is relatively high activity, there is no need to replace traditional ion sources for PET imaging. In contrast, it is desirable to think about innovative applications based on the strong points of z-pinches which are able to efficiently compress stored electrical energy in time and space. The potential of z-pinches, therefore, lies in the nanosecond duration of intense ion or neutron pulses. The application of z-pinches as ion sources is made difficult by debris escaping from a discharge. However, this is not a serious problem for fast neutrons which are able to penetrate through chamber walls, whereas troublesome debris produced by a z-pinch remains within an experimental chamber. Therefore, it seems natural to research z-pinches as nanosecond sources of neutrons. One of the possible applications is suggested in Sec. VI B.

### B. Fast-neutron radiograph with a nanosecond exposure

The previous paragraphs show that gas-puff z-pinches are able to produce a large number of ions within several nanoseconds. In order to demonstrate that also neutron numbers are sufficient for future applications, we tried to obtain the first z-pinch generated neutron radiograph. The scheme of an experimental set-up is shown in Figs. 11(a)–11(d). As a detector, we used two 1.2 mm thick CR-39 foils. The shielded CR-39 detector was placed behind various materials at the return-current cage, i.e., in the radial direction at

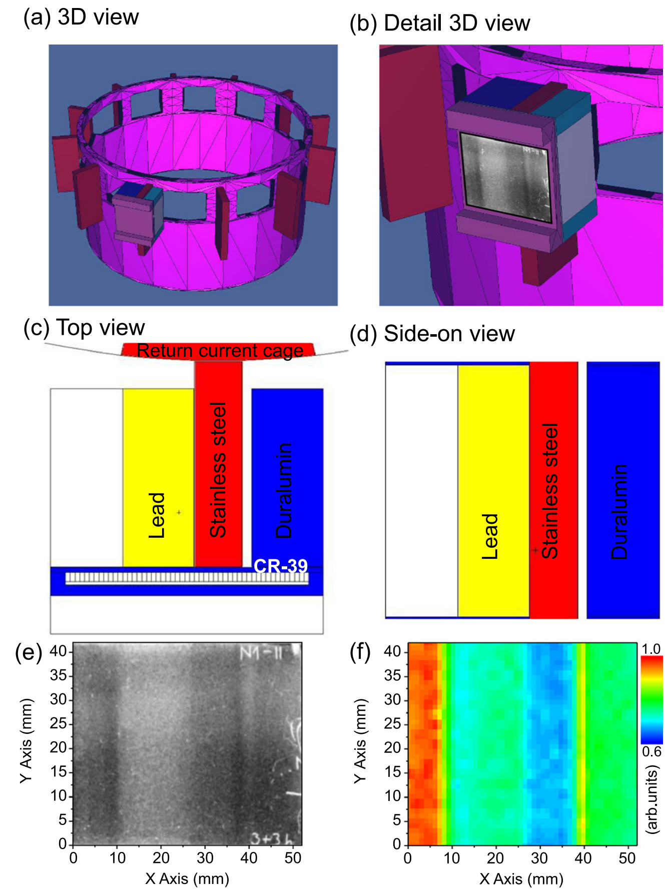


FIG. 11. Neutron radiography of 3.5 cm long, 4 cm high blocks of different materials. (a) Experimental arrangement, 3D view. (b) Experimental arrangement, detail 3D view. (c) Experimental arrangement, top view. (d) Experimental arrangement, side-on view. (e) Scan of the etched CR-39 detector, side-on view. (f) MCNP simulation of neutron fluence at the CR-39 detector, side-on view. The MCNP simulation was performed with a point neutron source with the spectrum from Ref. 19. It should be noted that the transparency of the CR-39 detector depended not only on the neutron fluence but also on neutron energies which were different behind each block.

25 cm from the neutron source. The advantage of the CR-39 nuclear track detector is that it is not sensitive to x-rays and electrons. Since all ions emitted in the radial direction were absorbed by 2 mm thick aluminum shielding, the CR-39 detector recorded only neutrons. The neutron detection efficiency of CR-39 material after etching is quite low, of the order of $10^{-4}$. In addition to that, the proton tracks are easily observable with the naked eye when there are more than 300 000 tracks per square cm$^2$. Therefore, to obtain a visible image at 25 cm, we accumulated neutrons from 20 shots with the total neutron yield of $3 \times 10^{13}$. The accumulation of 20 shots is not a limitation of our z-pinch. Since much more sensitive detectors are now available (e.g., Ref. 10), one neutron pulse generated by our z-pinch is essentially sufficient for neutron radiograph production. Besides that, the accumulation of 20 shots enables a rough estimate of the spatial fluctuation of a neutron source. The obtained experimental result is shown in Fig. 11(e). Even though the lengths of aluminum, lead, and stainless-steel blocks were only 3.5 or 4.0 cm, it is possible to see a quite contrast image which is in qualitative agreement with Monte Carlo N-Particle (MCNP) simulation.[36] By comparing Fig. 11(e) with Fig. 11(f), it can be

seen that all features observed in the experiment were reproduced by the MCNP simulation.

## VII. SUMMARY

In summary, we have presented the most important characteristics of the ion pulse generated by the novel configuration of the deuterium gas-puff z-pinch. We demonstrated that the gas-puff z-pinch on the GIT-12 generator is a powerful source of multi-MeV protons, deuterons, and neutrons. On the GIT-12 generator, multi-MeV ions were accelerated with a megaampere current. Since MA currents can be achieved with more compact, rep-rate drivers, which have become available,[55] our experimental results might be very important for many advanced applications. In this paper, we presented the first neutron radiograph generated by ≈20 ns pulses from the z-pinch. On the basis of our experiments, we further showed that a single shot would have been sufficient to obtain GBq positron activity of short-lived isotopes with a half-life in minutes. Even though these results are still far from commercial applications, it is evident that z-pinches may become unique sources of fast ions and neutrons.

The record values of ion energies and numbers do raise the question of what can be achieved at even higher currents? At this point, we should note that 100 kA z-pinches are able to generate up to 1 MeV deuterons,[56] whereas deuteron energies in MA z-pinches might exceed 10 MeV. Therefore, there is a good chance that optimized experiments at >10 MA currents could lead to breakthrough in z-pinch physics and applications. To provide an answer to the above mentioned question, better knowledge of acceleration mechanisms in z-pinches is required. This is precisely the area of our further research.

## ACKNOWLEDGMENTS

This research has been supported by the Grant Agency of the Czech Republic (Grant No. 16-07036S), the Czech Ministry of Education (Grant Nos. LD14089, LG13029, and LH13283), the Ministry of Education and Science of Russian Federation (Grant No. RFMEFI59114X0001), the IAEA (Grant No. RC17088), and the CTU (Grant No. SGS 16/223/OHK3/3T/13).

[1]R. B. Spielman, C. Deeney, G. A. Chandler, M. R. Douglas, D. L. Fehl, M. K. Matzen, D. H. McDaniel, T. J. Nash, J. L. Porter, T. W. L. Sanford, J. F. Seamen, W. A. Stygar, K. W. Struve, S. P. Breeze, J. S. McGurn, J. A. Torres, D. M. Zagar, T. L. Gilliland, D. O. Jobe, J. L. McKenney, R. C. Mock, M. Vargas, T. Wagoner, and D. L. Peterson, Phys. Plasmas **5**, 2105 (1998).
[2]Ye. P. Bogolubov, M. V. Koltunov, B. D. Lemeshko, V. I. Mikerov, V. N. Samosyuk, P. P. Sidorov, and D. I. Yurkov, Nucl. Instrum. Methods Phys. Res. A **605**, 62–64 (2009).
[3]M. V. Roshan, S. V. Springham, R. S. Rawat, and P. Lee, IEEE Trans. Plasma Sci. **38**, 3393 (2010).
[4]B. L. Bures, M. Krishnan, R. E. Madden, and F. Blobner, IEEE Trans. Plasma Sci. **38**, 667 (2010).
[5]V. A. Gribkov, S. V. Latyshev, R. A. Miklaszewski, M. Chernyshova, K. Drozdowicz, U. Wiacek, K. Tomaszewski, and B. D. Lemeshko, Phys. Scr. **81**, 035502 (2010).
[6]M. Krishnan, B. Bures, C. James, R. Madden, W. Hennig, D. Breus, S. Asztalos, K. Sabourov, and S. Lane, "A fast pulsed neutron source for time-of-flight detection of nuclear materials and explosives," AIP Conf. **1412**, 47–54 (2011).
[7]R. S. Rawat, Nanosci. Nanotechnol. Lett. **4**, 251–274 (2012).
[8]I. Spencer, K. W. D. Ledingham, R. P. Singhal, T. McCanny, P. McKenna, E. L. Clark, K. Krushelnick, M. Zepf, F. N. Beg, M. Tatarakis, A. E. Dangor, P. A. Norreys, R. J. Clarke, R. M. Allott, and I. N. Ross, Nucl. Instrum. Methods Phys. Res. Sect. B **183**, 449–458 (2001).
[9]S. Fritzler, V. Malka, G. Grillon, J. P. Rousseau, F. Burgy, E. Lefebvre, E. Dhumieres, P. McKenna, and K. W. D. Ledingham, Appl. Phys. Lett. **83**, 3039 (2003).
[10]M. Roth, D. Jung, K. Falk, N. Guler, O. Deppert, M. Devlin, A. Favalli, J. Fernandez, D. Gautier, M. Geissel, R. Haight, C. E. Hamilton, B. M. Hegelich, R. P. Johnson, F. Merrill, G. Schaumann, K. Schoenberg, M. Schollmeier, T. Shimada, T. Taddeucci, J. L. Tybo, F. Wagner, S. A. Wender, C. H. Wilde, and G. A. Wurden, Phys. Rev. Lett. **110**, 044802 (2013).
[11]D. Klir, J. Kravarik, P. Kubes, K. Rezac, S. S. Ananev, Yu. L. Bakshaev, P. I. Blinov, A. S. Chernenko, E. D. Kazakov, V. D. Korolev, B. R. Meshcherov, G. I. Ustroev, L. Juha, J. Krasa, and A. Velyhan, Phys. Plasmas **15**, 032701 (2008).
[12]Yu. L. Bakshaev, V. A. Bryzgunov, V. V. Vikhrev, I. V. Volobuev, S. A. Danko, E. D. Kazakov, V. D. Korolev, D. Klir, A. D. Mironenko-Marenkov, V. G. Pimenov, E. A. Smirnova, and G. I. Ustroev, Plasma Phys. Rep. **40**, 437–450 (2014).
[13]D. Klir, J. Kravarik, P. Kubes, K. Rezac, S. S. Ananev, Yu. L. Bakshaev, P. I. Blinov, A. S. Chernenko, E. D. Kazakov, V. D. Korolev, G. I. Ustroev, L. Juha, J. Krasa, and A. Velyhan, IEEE Trans. Plasma Sci. **37**, 425 (2009).
[14]D. Klir, J. Kravarik, P. Kubes, K. Rezac, J. Cikhardt, E. Litseva, T. Hyhlik, S. S. Ananev, Yu. L. Bakshaev, V. A. Bryzgunov, A. S. Chernenko, Yu. G. Kalinin, E. D. Kazakov, V. D. Korolev, G. I. Ustroev, A. A. Zelenin, L. Juha, J. Krasa, A. Velyhan, L. Vysin, J. Sonsky, and I. V. Volobuev, Plasma Phys. Controlled Fusion **52**, 065013 (2010).
[15]D. Klir, A. V. Shishlov, P. Kubes, K. Rezac, F. I. Fursov, V. A. Kokshenev, B. M. Kovalchuk, J. Kravarik, N. E. Kurmaev, A. Yu. Labetsky, and N. A. Ratakhin, Phys. Plasmas **19**, 032706 (2012).
[16]D. Klir, A. V. Shishlov, V. A. Kokshenev, P. Kubes, A. Yu. Labetsky, K. Rezac, J. Cikhardt, F. I. Fursov, B. M. Kovalchuk, J. Kravarik, N. E. Kurmaev, N. A. Ratakhin, O. Sila, and J. Stodulka, Plasma Phys. Controlled Fusion **55**, 085012 (2013).
[17]D. Klir, V. A. Kokshenev, P. Kubes, A. Labetsky, M. Paduch, K. Rezac, and A. Shishlov, IEEE Trans. Plasma Sci. **41**, 3129 (2013).
[18]D. Klir, P. Kubes, K. Rezac, J. Cikhardt, J. Kravarik, O. Sila, A. V. Shishlov, B. M. Kovalchuk, N. A. Ratakhin, V. A. Kokshenev, A. Yu. Labetsky, R. K. Cherdizov, F. I. Fursov, N. E. Kurmaev, G. N. Dudkin, B. A. Nechaev, V. N. Padalko, H. Orcikova, and K. Turek, Phys. Rev. Lett. **112**, 095001 (2014).
[19]D. Klir, A. V. Shishlov, V. A. Kokshenev, P. Kubes, A. Yu. Labetsky, K. Rezac, R. K. Cherdizov, J. Cikhardt, B. Cikhardtova, G. N. Dudkin, F. I. Fursov, A. A. Garapatsky, B. M. Kovalchuk, J. Kravarik, N. E. Kurmaev, H. Orcikova, V. N. Padalko, N. A. Ratakhin, O. Sila, K. Turek, and V. A. Varlachev, Plasma Phys. Controlled Fusion **57**, 044005 (2015).
[20]R. L. Gullickson and H. L. Sahlin, J. Appl. Phys. **49**, 1099 (1978).
[21]L. Bertalot, H. Herold, U. Jger, A. Mozer, T. Oppenlnder, M. Sadowski, and H. Schmidt, Phys. Lett. A **79**, 389392 (1980).
[22]A. Mozer, M. Sadowski, H. Herold, and H. Schmidt, J. Appl. Phys. **53**, 2959 (1982).
[23]W. H. Bostick, H. Kilic, V. Nardi, and C. W. Powell, Nucl. Fusion **33**, 413 (1993).
[24]D. R. Welch, D. V. Rose, C. Thoma, R. E. Clark, C. B. Mostrom, W. A. Stygar, and R. J. Leeper, Phys. Plasmas **17**, 072702 (2010).
[25]M. G. Haines, Plasma Phys. Controlled Fusion **53**, 093001 (2011).
[26]S. P. Bugaev, A. M. Volkov, A. A. Kim, V. N. Kiselev, B. M. Kovalchuk, N. F. Kovsharov, V. A. Kokshenev, N. E. Kurmaev, S. V. Loginov, G. A. Mesyats, F. I. Fursov, and A. P. Khuzeev, Russ. Phys. J. **40**, 1154–1161 (1997).
[27]J. Krasa, M. Kralik, A. Velyhan, J. Solc, L. Juha, M. Scholz, B. Bienkowska, I. M. Ivanova-Stanik, L. Karpinski, R. Miklaszewski, M. Paduch, H. Schmidt, K. Tomaszewski, D. Klir, J. Kravarik, P. Kubes, and K. Rezac, Plasma Phys. Controlled Fusion **50**, 125006 (2008).
[28]M. B. Chadwick, P. Oblozinsky, M. Herman, N. M. Greene, R. D. McKnight, D. L. Smith, P. G. Young, R. E. MacFarlane, G. M. Hale, S. C. Frankle, A. C. Kahler, T. Kawano, R. C. Little, D. G. Madland, P. Moller, R. D. Mosteller, P. R. Page, P. Talou, H. Trellue, M. C. White, W. B. Wilson, R. Arcilla, C. L. Dunford, S. F. Mughabghab, B. Pritychenko, D.

Rochman, A. A. Sonzogni, C. R. Lubitz, T. H. Trumbull, J. P. Weinman, D. A. Brown, D. E. Cullen, D. P. Heinrichs, D. P. McNabb, H. Derrien, M. E. Dunn, N. M. Larson, L. C. Leal, A. D. Carlson, R. C. Block, J. B. Briggs, E. T. Cheng, H. C. Huria, M. L. Zerkle, K. S. Kozier, A. Courcelle, V. Pronyaev, and S. C. van der Marck, Nucl. Data Sheets **107**, 2931 (2006).
[29]H. Ing, Radiat. Meas. **33**, 275–286 (2001).
[30]F. C. Young, J. Golden, and C. A. Kapetanakos, Rev. Sci. Instrum. **48**, 432 (1977).
[31]D. T. L. Jones and C. M. Bartle, Nucl. Instrum. Methods **118**, 525–529 (1974).
[32]F. C. Young, D. Mosher, S. J. Stephanakis, and S. A. Goldstein, Phys. Rev. Lett. **49**, 549 (1982).
[33]D. Klir, J. Kravarik, P. Kubes, K. Rezac, E. Litseva, K. Tomaszewski, L. Karpinski, M. Paduch, and M. Scholz, Rev. Sci. Instrum. **82**, 033505 (2011).
[34]J. F. Ziegler, Nucl. Instrum. Methods B **219–220**, 1027 (2004).
[35]M. Schollmeier, M. Geissel, A. B. Sefkow, and K. A. Flippo, Rev. Sci. Instrum. **85**, 043305 (2014).
[36]T. Goorley, M. James, T. Booth, F. Brown, J. Bull, L. J. Cox, J. Durkee, J. Elson, M. Fensin, R. A. Forster, J. Hendricks, H. G. Hughes, R. Johns, B. Kiedrowski, R. Martz, S. Mashnik, G. McKinney, D. Pelowitz, R. Prael, J. Sweezy, L. Waters, T. Wilcox, and T. Zukaitis, Nucl. Technol. **180**, 298–315 (2012).
[37]M. Krishnan, IEEE Trans. Plasma Sci. **40**, 3189 (2012).
[38]S. P. Hatchett, C. G. Brown, T. E. Cowan, E. A. Henry, J. S. Johnson, M. H. Key, J. A. Koch, A. B. Langdon, B. F. Lasinski, R. W. Lee, A. J. Mackinnon, D. M. Pennington, M. D. Perry, T. W. Phillips, M. Roth, T. C. Sangster, M. S. Singh, R. A. Snavely, M. A. Stoyer, S. C. Wilks, and K. Yasuike, Phys. Plasmas **7**, 2076 (2000).
[39]S. C. Wilks, A. B. Langdon, T. E. Cowan, M. Roth, M. Singh, S. Hatchett, M. H. Key, D. Pennington, A. MacKinnon, and R. A. Snavely, Phys. Plasmas **8**, 542 (2001).
[40]H. Daido, M. Nishiuchi, and A. Pirozhkov, Rep. Prog. Phys. **75**, 056401 (2012).
[41]A. G. Krygier, J. T. Morrison, S. Kar, H. Ahmed, A. Alejo, R. Clarke, J. Fuchs, A. Green, D. Jung, A. Kleinschmidt, Z. Najmudin, H. Nakamura, P. Norreys, M. Notley, M. Oliver, M. Roth, L. Vassura, M. Zepf, M. Borghesi, and R. R. Freeman, Phys. Plasmas **22**, 053102 (2015).
[42]M. I. K. Santala, M. Zepf, F. N. Beg, E. L. Clark, A. E. Dangor, K. Krushelnick, M. Tatarakis, I. Watts, K. W. D. Ledingham, T. McCanny, I. Spencer, A. C. Machacek, R. Allott, R. J. Clarke, and P. A. Norreys, Appl. Phys. Lett. **78**, 19 (2001).
[43]S. Kar, A. Green, H. Ahmed, A. Alejo, A. P. L. Robinson, M. Cerchez, R. Clarke, D. Doria, S. Dorkings, J. Fernandez, S. R. Mirfyazi, P. McKenna, K. Naughton, D. Neely, P. Norreys, C. Peth, H. Powell, J. A. Ruiz, J. Swain, O. Willi, and M. Borghesi, e-print arXiv:1507.04511.
[44]D. Jung, K. Falk, N. Guler, O. Deppert, M. Devlin, A. Favalli, J. C. Fernandez, D. C. Gautier, M. Geissel, R. Haight, C. E. Hamilton, B. M. Hegelich, R. P. Johnson, F. Merrill, G. Schaumann, K. Schoenberg, M. Schollmeier, T. Shimada, T. Taddeucci, J. L. Tybo, S. A. Wender, C. H. Wilde, G. A. Wurden, and M. Roth, Phys. Plasmas **20**, 056706 (2013).
[45]S. Humphries, Nucl. Fusion **20**, 1549–1612 (1980).
[46]P. J. VanDevender and D. L. Cook, Science **232**, 831–836 (1986).
[47]R. A. Meger, F. C. Young, A. T. Drobot, G. Cooperstein, S. A. Goldstein, D. Mosher, S. E. Graybill, G. A. Huttlin, K. G. Kerris, and A. G. Stewart, J. Appl. Phys. **52**, 6084 (1981).
[48]D. D. Hinshelwood, P. F. Ottinger, J. W. Schumer, R. J. Allen, J. P. Apruzese, R. J. Commisso, G. Cooperstein, S. L. Jackson, D. P. Murphy, D. Phipps, S. B. Swanekamp, B. V. Weber, and F. C. Young, Phys. Plasmas **18**, 053106 (2011).
[49]T. J. Renk, V. Harper-Slaboszewicz, K. A. Mikkelson, W. C. Ginn, P. F. Ottinger, and J. W. Schumer, Phys. Plasmas **21**, 123114 (2014).
[50]K. W. D. Ledingham, P. McKenna, T. McCanny, S. Shimizu, J. M. Yang, L. Robson, J. Zweit, J. M. Gillies, J. Bailey, G. N. Chimon, R. J. Clarke, D. Neely, P. A. Norreys, J. L. Collier, R. P. Singhal, M. S. Wei, S. P. D. Mangles, P. Nilson, K. Krushelnick, and M. Zepf, J. Phys. D: Appl. Phys. **37**, 2341–2345 (2004).
[51]S. Kimura and A. Bonasera, Nucl. Instrum. Methods Phys. Res. Sect., A **637**, 164–170 (2011).
[52]A. Maksimchuk, A. Raymond, F. Yu, G. M. Petrov, F. Dollar, L. Willingale, C. Zulick, J. Davis, and K. Krushelnick, Appl. Phys. Lett. **102**, 191117 (2013).
[53]T. C. Rust, E. V. R. DiBella, C. J. McGann, P. E. Christian, J. M. Hoffman, and D. J. Kadrmas, Phys. Med. Biol. **51**, 5347–5362 (2006).
[54]K. W. D. Ledingham and W. Galster, New J. Phys. **12**, 045005 (2010).
[55]M. G. Mazarakis, W. E. Fowler, K. L. LeChien, F. W. Long, M. K. Matzen, D. H. McDaniel, R. G. McKee, C. L. Olson, J. L. Porter, S. T. Rogowski, K. W. Struve, W. A. Stygar, J. R. Woodworth, A. A. Kim, V. A. Sinebryukhov, R. M. Gilgenbach, M. R. Gomez, D. M. French, Y. Y. Lau, J. C. Zier, D. M. VanDevalde, R. A. Sharpe, and K. Ward, IEEE Trans. Plasma. Sci. **38**, 704 (2010).
[56]A. Schmidt, V. Tang, and D. Welch, Phys. Rev. Lett. **109**, 205003 (2012).